ELSEVIER
Available online at www.sciencedirect.com
ScienceDirect
Transportation Research Procedia 10 (2015) 82 – 92
Transportation Research Procedia
www.elsevier.com/locate/procedia

18th Euro Working Group on Transportation, EWGT 2015, 14-16 July 2015, Delft, The Netherlands

Mesoscopic traffic state estimation based on a variational formulation of the LWR model in Lagrangian-space coordinates and Kalman filter

Yufei Yuan [a,*], Aurélien Duret [b], Hans van Lint [a]

[a] *Delft University of Technology, Stevinweg 1, 2628CN, Delft, The Netherlands*
[b] *IFSTTAR, LICIT, F-69675, Bron Cedex, France*

Abstract

This paper proposes a new model-based traffic state estimation framework using the LWR model formulated in vehicle number – space (Lagrangian – space) coordinates. This formulation inherits the numerical benefits and modelling flexibility from Lagrangian (vehicle number – time) models. Specifically, a variational formulation of the LWR model is selected as the underlying process model. Compared to the traditional conservation law approach in the same coordinate system, the current formulation entitles a simplified expression (no complex state updating originated from different traffic conditions), and provides more accurate numerical results in the prediction step of the data assimilation framework (exact solution to the continuous model when the fundamental diagram is bi-linear). More importantly, this formulation is particularly convenient for data assimilation, because in reality, the flow characteristics are mostly observed at fixed point (spatial fixed) or along vehicle trajectories (vehicle number fixed). These observations are located on cell boundaries of the Lagrangian-space grid, which makes any traffic state estimation method convenient with this approach. Its corresponding observation models are also defined to incorporate both spatial-fixed and moving observations. A Kalman filter framework is applied with the underlying traffic system model. Moreover, travel time can be directly derived from system estimates, and no state transformation is required compared to other estimation approaches. Model validation experiment based on a synthetic traffic network has demonstrated the feasibility of the proposed framework, and suggested promising extensions for future applications.

Peer-review under responsibility of Delft University of Technology

Keywords: Traffic state estimation; variational formulation; LWR model; Lagrangian-space coordinates; Kalman filter

1. Introduction

* Corresponding author. Tel.: +31-15-27-86304; fax: +31-15-27-379
E-mail address: y.yuan@tudelft.nl

Peer-review under responsibility of Delft University of Technology
doi:10.1016/j.trpro.2015.09.058

Traffic state estimation (TSE) and short-term state forecasting are central components in dynamic traffic management and information applications. Generally model-based TSE relies on two components: a model-based component and a data assimilation algorithm. The model-based component consists of two parts: a) a dynamic traffic flow model to predict the evolution of the state variables; and b) a set of observation equations relating sensor observations to the system state. Thereafter, a data-assimilation technique is adopted to combine the model predictions with the sensor observations. For example, the Kalman filter (KF) (Herrera and Bayen (2010)) and it advanced relatives, such as Extended KF (Wang and Papageorgiou (2005)), Unscented KF (Ngoduy (2008)), Ensemble KF (Work *et al.* (2008)) have been widely applied in the field of traffic state estimation.

The same traffic flow model can be formulated in three two-dimensional coordinate systems regarding space x, time t and vehicle number n. Laval and Leclercq (2013) have presented three equivalent variational formulations of the first-order traffic flow models, namely $N(x,t)$ model, $X(t,n)$ model, $T(n,x)$ model respectively, under the theory of Hamilton-Jacobi partial differential equations. Most of TSE applications are based on the traditional space-time (Eulerian) formulation. Recent studies have shown that a first-order (LWR) traffic flow model can be formulated and solved more efficiently and accurately in vehicle number–time (Lagrangian) coordinates (Leclercq *et al.* (2007)). And its related Lagrangian formulation of state estimation enables more accurate and efficient application of data assimilation methods, due to the solution to the mode-switching problem (traffic information travels in one direction) and less non-linearity of the system model (Yuan *et al.* (2012)).

Furthermore, Yang *et al.* (2015) have investigated the possibility for TSE in the vehicle number-space coordinate systems. Their formulation follows a traditional conservation law approach. The conservation law equation is discretized, and traffic pace is used as the state updating variable. Due to the retainment of spatial coordinates (preserve segment-based representation), traffic information still travels in both directions. This formulation still requires complex state updating matrix for various traffic conditions (upwind and downwind numerical schemes considering both downstream and upstream cells), which is the same as the Eulerian counterpart. The numerical benefit from Lagrangian models is not fully achieved. As argued in Yuan *et al.* (2012), small disturbance for state estimation around capacity point may result in corrections with the “wrong” sign (i.e., the estimator may infer congested traffic while in reality traffic is flowing freely). Alternatively, TSE relied on a variational (Hamilton-Jacobi) formulation of traffic flow models is considered to be much simpler to compute and numerically more accurate under same conditions, compared with the conservation law approach. However, only a few studies have applied such formulations for state estimation purposes. As one of the few examples, Deng *et al.* (2013) extended Newell’s three-detector model (the aforementioned N-model, Newell (1993)) for TSE. It provided a more flexible way to assimilate real-world heterogeneous data sources compared to the Eulerian conservation law approach.

This paper proposes a novel mesoscopic model-based traffic state estimation framework using a variational formulation of the LWR model in vehicle number – space (Lagrangian-space) coordinates. This formulation can incorporate the numerical benefits and modelling flexibility of Lagrangian-time models. Specifically, the variational formulation of the LWR model is selected as the underlying process model. Compared to the traditional conservation law approach in the same coordinate system, the current formulation entitles a simplified expression (no complex state updating originated from different traffic conditions), and provides more accurate numerical results in the prediction step of the data assimilation framework (exact solution to the continuous model when the fundamental diagram is bi-linear). Its corresponding observation models are also included to incorporate both spatial-fixed and moving observations. A Kalman filter framework with the underlying model is proposed, and it will be validated on a synthetic network, namely a homogeneous corridor with boundary conditions.

This paper is organized as follows. Section 2 presents the methodology of the proposed TSE framework, including underlying traffic flow model, corresponding observation models and the data assimilation technique. Section 3 illustrates the experimental setup. Loop and probe vehicle data are generated from a synthetic traffic network. Different scenarios are defined to validate the framework under selected performance indicators. Section 4 summarizes the simulation results. Conclusions and recommendations are drawn in Section 5.

2. Methodology

This section defines both the process model and observation models in the state estimation framework. Due to the linear formulation of the traffic system, a linear Kalman filter is used as the data assimilation technique.

2.1. General formulation of the LWR model in Lagrangian-space coordinates

This section first presents a mesoscopic formulation of the LWR model as the process model in the estimation framework. The LWR model is formulated in vehicle platoon and space (n, x) coordinates, named as Lagrangian-space coordinates throughout the paper. The term mesoscopic is in response to the two other counterparts, since the Lagrangian-time coordinates can apply in a microscopic simulation framework and the Eulerian coordinates can accommodate in a macroscopic one. The current mesoscopic formulation combines a vehicular description with macroscopic behavioral rules. It relaxes the temporal coordinate, and this entitles a transformation of a temporal progressing approach (e.g., in Eulerian or Lagrangian-time simulation framework) to an event-progressing approach (trigger event can be the change of time headway or pace, and/or a correction procedure based on an observation from fixed loops or probe vehicles).

The formulation follows the principle of the Hamilton-Jacobi (HJ) theory, to find an expression of the LWR model in Lagrangian-space coordinates. Let h denote the time headway, Q and V denote traffic flow and speed, and $h = 1/Q$. In the Lagrangian-space coordinates (n, x), the LWR model can then be described by a hyperbolic equation:

$$\partial_x h - \partial_N (1/V(h)) = 0 \quad (1)$$

Previous authors have proposed to apply variational theory in Eulerian coordinates (x, t) (Daganzo (2005)) and Lagrangian coordinates (n, t) (Leclercq *et al.* (2007)). Here, we transpose the demonstration in Lagrangian-space coordinates (n, x), following the same rationale in Leclercq *et al.* (2007). The problem can also be expressed in terms of $T(n, x)$ considering the "passage time" flux that crosses the boundary of the cell n, specifically it is expressed as the Hamilton-Jacobi derived from the fundamental diagram:

$$\partial_x T = \frac{1}{V(\partial_n T)} \quad (2)$$

Here, the function $1/V$ represents the flux function of the problem. This model is also referred to as the T-model. Here, we consider a triangular fundamental with three parameters: the free-flow speed v_m, the maximum wave speed w and the jam density k_x. It can be expressed by:

$$\frac{1}{V(h)} = max\left(1/v_m, -k_x.(\frac{1}{w.k_x} - h)\right) \quad (3)$$

We apply a variational formulation of the T-model. The numerical solution to the Hamilton-Jacobi formulation, under the assumption of a CFL condition with an equality condition (namely, $\Delta n = \Delta x k_x$) and a triangular fundamental relation, reads as follow:

$$T(n, x) = max\left(T(n, x - \Delta x) + \frac{\Delta x}{v_m}, T(n - \Delta n, x + \frac{\Delta n}{k_x}) + \frac{\Delta n}{w.k_x}\right) \quad (4)$$

The complete demonstration can refer to Leclercq (2007), and Laval and Leclercq (2013).

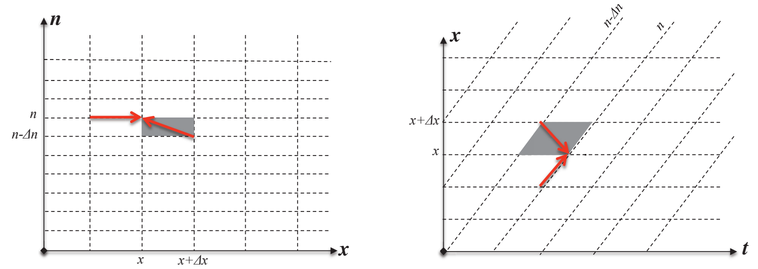

Fig. 1. Numerical solutions in Lagrangian-space coordinates

The formulation refers to as the so-called "lattice" implementation of the continuous T-model. In this form, the coordinate system is discrete but with the continuous dependent variable (passage time: T) (Laval and Leclercq (2013)). Specifically, traffic flow on a freeway stretch is divided into vehicle platoons of size Δn, and road stretch is discretized with spatial cells of length Δx. The solution is illustrated by Fig. 1 (see arrow directions). This variational form still preserves the segment-based representation as in the Eulerian counterpart. Unlike a traditional conservation law approach presented in Yang *et al.* (2015), there is no complex state evolution to account for different traffic conditions (information propagation directions), instead it always involves comparing only two uncorrelated terms.

The variational formulation can provide more accurate results in the prediction step of the estimation framework (exact solution to the continuous model when the fundamental diagram is bi-linear). More importantly, it simplifies the formulation with only one expression to consider all different traffic conditions, which is beneficial for efficient data assimilation framework.

2.2. Observation models in Lagrangian-space coordinates

In Lagrangian-space coordinates, observation equations are defined to relate sensor observations with system states. The flow characteristics are mostly observed at fixed points (x fixed) or along vehicle trajectories (n fixed). These observations are located on cell boundaries of the mesoscopic grid.

From empirical data, it is however difficult to address a particular observation (passage time) to a certain vehicle platoon (with index n) at a given location (x), since the vehicle numbering in the numerical model is not traceable by loop detection systems or by probe vehicles. The index of vehicles that pass by loops or probe vehicles is unknown. If this information were known (e.g., the cumulative vehicle count (CVC) of a loop is available, the ID of a particular probe in the model is known), it would be a direct observation of the current estimated state.

Normally from loop detection systems, aggregate flow (time headway h_{obs}) and speed (pace τ_{obs}) information at a given time period (e.g., 60s) can be obtained. For floating car data (FCD), the updating location, speed sample and the relating time instant are available; or even travel time (TT_{obs}) of a particular probe vehicle is known. Also in the model, the states (passage time) of the leading platoon ($n - \Delta n$) are estimated from the previous "platoon" step; the state of the current platoon at previous location ($x - \Delta x$) can be estimated in advance in the current calculation horizon. With this information, we can derive observation models under the assumption of homogeneous conditions of a small space-vehicle platoon (or space-time) region. Here, it is assumed that direct observations of system states at the current estimation step can be obtained under the aforementioned assumptions. Four observation models with single data source are defined:

$$\text{(a)}\quad T_{obs}(n,x) = T(n,x) + r_n = T(n-\Delta n, x) + \Delta n \cdot h_{obs}(n-\Delta n, x) \tag{5}$$

Here, r_n denotes the white noise terms in the observation model. h_{obs} can be obtained from the loop measurement at location x (or the adjacent location) and time $T(n-\Delta n, x)$.

$$\text{(b)}\quad T_{obs}(n,x) = T(n,x) + r_n = T(n, x-\Delta x) + \Delta x \cdot \tau_{obs}(n, x-\Delta x) \tag{6}$$

In this observation equation, τ_{obs} can be obtained from the loop measurement at location $x - \Delta x$ (or the adjacent location) and time $T(n, x-\Delta x)$. Alternatively, it can be obtained from a probe vehicle report at location $x - \Delta x$ and time $T(n, x-\Delta x)$ (or the adjacent spatio-temporal area)

$$\text{(c)}\quad T_{obs}(n,x) = T(n,x) + r_n = T(n, x-\Delta x) + TT_{obs}(n, x-\Delta x) \tag{7}$$

Travel time can be obtained from a probe vehicle travelling from location $x - \Delta x$ and time $T(n, x-\Delta x)$ (or the adjacent spatio-temporal area) to location x.

$$\text{(d)}\quad T_{obs}(n,x) = T(n,x) + r_n \tag{8}$$

If the CVC of a loop at location x is known, or a particular probe can be related to a vehicle-platoon n in the model, this observation equation applies.

2.3. TSE based on Kalman filter

Now we have defined both the process model and observation models. Generally for real applications, traffic flow models are not fully reliable (due to the misspecification of reality and errors in model parameters.) neither for the observations (which contain measurement errors). The essence of data assimilation techniques is to balance the weights on the model and observation, and to infer an optimal estimate of traffic states. Therefore, we need to consider error terms in both process equations and observation equations. The traffic state estimation procedure is presented as follows and illustrated by Fig. 2.

a. Initialize the states (vehicle passage time) at two boundaries “$x = 1$” and “$n = 1$”. That means that the CVCs at the entry of the link (e.g., provided by a loop) and the trajectory of the first vehicle (e.g., provided by a probe). Note that the states at boundaries do not necessarily have to be accurate.
b. The model applies an explicit vehicle-platoon progressing approach. That means the states of the consecutive platoons (n =2, 3, 4, …) over the whole spatial dimension are updated according to the process model. The process and observation models are linearly formulated; therefore, standard linear KF (Kalman (1960)) can be applied to perform data assimilation.
c. Prediction step:
Process model to calculate prior system states:

$$T(n,x) = max\left(T(n,x-\Delta x) + \frac{\Delta x}{v_m}, T(n-\Delta n, x+\Delta x) + \frac{\Delta x}{w}\right) + \sigma_n \tag{9}$$

Here, σ_n denotes the white noise terms in the process model. The model error covariance matrix needs to define. This discrete form allows a state-by-state evolution for a particular vehicle platoon. The red arrows in Fig. 2 show the prediction step for a particular platoon (n) at a specific location (x).

d. Correction step:
In the correction step, observations are used to correct the prior state prediction. The Kalman gain (K) is determined. And posterior states and error covariance matrix are updated. In Fig. 2, blue arrows indicate three possible ways of incorporating observations, corresponding to observation models (a), (b) and (c).

e. End of one iteration.

Let us recap the standard linear KF procedure. It consists of the prediction step and the correction step. Here the system state is expressed by passage time of a particular platoon n at a specific location x: $\hat{X}_k = T(n,x)$.

- *Prediction step*:

The KF model assumes the true state at step k is evolved from the state at step $k-1$ according to a so-called prior state estimate:

$$\hat{X}_{k|k-1} = F_k \hat{X}_{k-1|k-1} + B_{k-1} u_{k-1} \tag{10}$$

In the current linear formulated system model: $F_k = 1$, it is the state transition model which is applied to the previous state. $B_{k\text{-}1}$ is the control-input model which is applied to the control vector $u_{k\text{-}1}$. A prior for the error covariance is computed by:

$$P_{k|k-1} = F_k P_{k-1|k-1} {F_k}^T + Q_k \tag{11}$$

Here, Q_k represents the covariance matrix associated with the Gaussian noise term σ_n in the process model (16).

- *Correction step*:

The Kalman gain K determines the optimal weight put on both the model-predicted state and observation input. It is calculated on the basis of two error covariances: observation covariance and system state covariance. It reads:

$$K_k = \frac{P_{k-1|k-1} {H_k}^T}{H_k P_{k-1|k-1} {H_k}^T + R_k} \tag{12}$$

Here, R_k depicts the covariance matrix of the Gaussian noise term r_n in observation models (12-15). Then the posterior state estimate and posterior error covariance are given by:

$$\hat{X}_{k|k} = \hat{X}_{k|k-1} + K_k (Z_k - H_k \cdot \hat{X}_{k|k-1}) \tag{13}$$

$$P_{k|k} = (I - K_k \cdot H_k) P_{k|k-1} \tag{14}$$

Here, Z_k denotes the observation made at step k; H_k is the observation model which maps the true state (prior state estimate) into the observation. $H_k = 1$ or $[1; 1]$, because the observation here is directly related to the state.

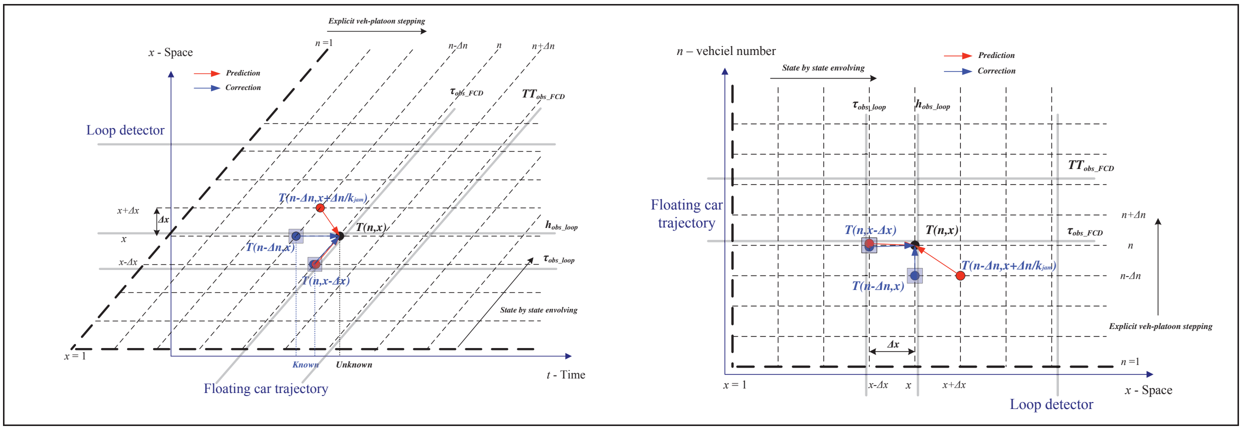

Fig. 2. Illustration of the mesoscopic traffic state estimation concept in two coordinate systems.

2.4. Advantages of the proposed state estimation formation

The current mesoscopic formulation is based on the notions from the variational theory. It can incorporate the numerical benefits and modelling flexibility of Lagrangian-time models. Simultaneously, this formulation allows state distinction on both link class and vehicle class, combining a vehicular description with macroscopic behavioral rules. The state process model applies a lattice implementation of the Lagrangian-space model. It individually represents vehicles (platoons) but only tracks their states (passage times) at link/cell boundaries. Therefore, travel time can be easily derived from the model, which is convenient compared to other (e.g., Eulerian or Lagrangian) formulations of state estimation. This discrete model evolves state by state, with only one expression to consider all traffic conditions. Hence, it does not require memory and more flexible and time-efficient for data assimilation (no complex matrix inversion and multiplication). In addition, the selected triangular fundamental diagram allows the numerical solution to become exact to the continuous form in the HJ framework, whereas this is not the case in the traditional conservation law approach (see, Laval and Leclercq (2013), LeVeque (1992), Yang *et al.* (2015)).

More importantly, this scheme is particularly convenient for state estimation, because in reality, the flow characteristics are mostly observed at fixed point (spatial fixed) or along vehicle trajectories (vehicle-number fixed). These observations are located on cell boundaries of the mesoscopic grid, which makes any traffic state estimation method convenient with this approach. Meanwhile, the derived observation models allow incorporating any type of observations: *a*) observations with exact indexing of vehicles/probes, such as the current probe vehicle relates to which platoon in the estimation model and cumulative vehicle counts at a loop detector; *b*) observations with unknown indexing, such as aggregate loop data and general form of floating car data.

This formulation can be easily coupled with any data assimilation techniques to perform state estimation. Due to the nature of the mesoscopic system model, the TSE might be not restricted to discretized mesoscopic $X - N$ grids. If we know any two boundaries in the network and an observation at a certain location, we can generalize TSE for this specific location.

3. Experiment setup and model validation

3.1. Data and test network

To validate the proposed state estimation framework, we perform a simulation study. A homogeneous corridor with boundary conditions is selected; it is a one-lane road stretch of 1000 m in length. Note that for validation purposes, the current network scale is sufficient to demonstrate the performance of the estimation framework. Traffic states on this corridor are various from free-flowing to highly congested traffic condition. Model verification is performed with respect to synthetic data generated by the Newell's car-following model and the same traffic conditions in the same road network. The logic is to let the Newell's car following model, which is consistent/equivalent with the LWR model at a macroscopic scale, provide individual vehicle trajectories. Based on the ground-truth trajectories, we can emulate any type of observation data and define different scenarios to test the performance of the estimator.

The total simulation time period is 1000 s. The fundamental diagram is bi-linear, with three parameters: the free-flow speed $v_m = 20\text{m/s}$, the maximum wave speed $w = 5\text{m/s}$ and the jam density $k_x = 0.17\text{veh/m}$. For the numerical scheme, the size of platoon Δn is chosen as 1, and thus individual vehicle can be tracked. The CFL condition is satisfied as an equality, thus the spatial cell size becomes $\Delta x = \Delta n / k_x \approx 5.88\text{m}$. The choice of the grid size depends on the trade-off between the numerical accuracy and computational cost.

In the linear Kalman filter framework, all the error terms are assumed to be zero-mean Gaussian distributed. The error covariance matrices Q and R relate to the uncertainty in process and observation models respectively. The Kalman gain depends on the ratio of error terms in these two matrices. Given a fixed Q, if the uncertainty in the observation model is small, then R tends to be small and thus the gain is large. That means the learning rate from observations is high, and vice versa. An appropriate combination of Q and R is important for providing good estimates. A Monte-Carlo simulation technique can be used to obtain a proper combination. For the sake of brevity, the results of the combination (Q: 5^2, R: 2^2) leading to the highest performance in estimation are presented in this paper.

3.2. Experimental scenarios

Several scenarios have been performed to test validity of the model framework as well as the corresponding observation models with diverse detection resolutions.

In practice, detectors are placed 500m by 60s apart on average, e.g., in the Netherlands. Under the current condition, the size of the network (1000m) and time span (1000s) allows only 2 detectors and 16 observation instants. Therefore, the setup of the observation (probably the prediction model) is adjusted to enable more observations. The virtual detectors are placed at every 100m (150m) and aggregate flows and speeds over 10s. The same logic applies to the FCD data. The enable more observations, the updating interval of FCD is set as 5s. Be aware of that, the extension of network scale would only increase computational cost but it gives no implication for estimation complexity.

Five observation models are tested: three with exclusive data sources and two with mixture of data sources. We consider flow and speed measurements from loop detectors with varying spatial resolutions, and speeds from probe vehicles with varying penetration rates. In this case, we do not need to know the exact indexing of observers (at loops or from FCD) in the corresponding estimation model. Meanwhile, when two data sources are available for one estimation grid, probe vehicle data are assumed to be more reliable than aggregate loop data (which is the case in reality), and thus overrule the loop data. Three testing levels for each case allow testing performance regarding detection resolutions. Table 1 provides an overview of all the testing scenarios.

Table 1. Experimental scenarios with five observation cases and three testing levels.

Obs. Model (scenario)	Data source	Resolution (testing level) (spacing and/or penetration)	No. runs (10 for each scenario)
1	Loop flow	100m, 150m, 200m	30
2	Loop speed	100m, 150m, 200m	30
3	FCD speed	15%, 10%, 5%	30
4	Loop flow FCD speed	150m&15%, 150m&10%, 200m&%5	30
5	Loop speed FCD speed	150m&15%, 150m&10%, 200m&%5	30

In addition, we performed a sensitivity analysis with respect to model input and observation input. Three types of sensitivity test scenarios were performed with the five observation models (testing level two). First, random errors (Gaussian noise) were added into observation inputs (loop aggregation data and probe vehicle data). Second, random errors were put into initial (spatial) boundary conditions. Third, structural errors were introduced in fundamental relations, by defining different parameters compared to the ground truth data.

In each of the testing scenarios, 10 simulation runs with different traffic patterns (different upstream and downstream boundaries of the homogeneous corridor) have been performed to account for stochastic effects.

3.3. Performance indicator

To assess different scenarios, performance criteria must be specified. The estimates from the state estimator are passage times of specific platoons at given locations (cell boundaries). To facilitate result comparison, first both these estimates and ground-truth trajectory data are transformed into system states (traffic density k, traffic speed v) in equidistant spatio-temporal grids (20 m x 20 s) in Eulerian coordinates under Edie's definition (Edie (1965)), and travel time TT at selected locations (every 200 m in the corridor - starting at 100m). Then, the estimates (u – denote either k or v) are compared with the ground truth (reference $\hat{u}$) data in terms of root mean square error ($RMSE$) and mean absolute percentage error ($MAPE$). Both error indicators can provide absolute and relative performance of estimation scenarios. They read:

$$RMSE = \sqrt{\frac{\sum(u-\hat{u})^2}{NN}} \quad (15) \qquad MAPE = \frac{1}{NN}\sum\frac{|u-\hat{u}|}{\hat{u}} \quad (16)$$

where NN denotes the total number of estimates.

4. Result and discussion

4.1. *Quantitative result*

Table 2 and Table 3 present the error indicators of state estimation with different observation models. Clearly, state estimation accuracy increases with detection resolutions (from testing level 1 to 3).

The TSE provides satisfactory results with loop-flow data (Obs1). The reason for that is twofold: (a) the most upstream loop detectors render a robust estimation of the flow demand on the link/cells (regarding demand time) and (b) the loops along the section gives a robust estimation of the supply/congested states (regarding supply time). The resulting traffic relies on the result of the competition between demand and supply; therefore, it is not surprising to obtain good performance with loop detectors only. In the current framework, traffic states are estimated at specific points of the section and then the model propagates demands in the downstream direction while supplies propagate upstream. It should be noted that if a loop detector were missing at the beginning (respectively the end) of the link, the flow demand (supply) would not be properly estimated and the performance of the TSE method upstream the first loop (downstream the last) detector of the section would be poor. In the current experimental setup, no exit detector of the section (at 1000m) is given, thus the estimation at the downstream boundary is not sufficient (as illustrated in Fig. 3).

The TSE with loop-speed data (Obs2) provides comparable results as the first case and the reason is the similar to observation model 1. The upstream demand is still given by the boundary condition. It is supplemented by the internal loop-speed observations that give a robust estimation of the congested/supply states within the link. It is also noticed that for travel time estimation, observation model 2 outperforms all the other observation models in terms of relative errors (Table 3).

The results with purely FCD (Obs3) are rather limited compared to Observation models 1 and 2. When loop detectors capture 100% of the flow passing over the loop, even with an optimistic rate of equipped vehicles (10%), FCD only provide one-off (isolated) position-speed measures with hazardous time-space coverage. Moreover, in presence of stop-and-go waves, FCD position-speed measures may not be representative of the average traffic state. Consequently, FCD alone cannot provide satisfactory traffic state estimation when a link presents saturated flows. The poor quality of the TSE is even more acute looking at the travel time estimation.

The main weakness of loop data is not to be able to capture congestion downstream the detector location. To mitigate this shortcoming, the observation can be supplemented by other data. Probe data are natural contenders to complete the data provided by loop. They provide accurate position-speed measurement in real-time with uniform spatial coverage of the network. However, the penetration rate is generally low (<10% in reality) and cannot provide an accurate estimation of the demand level. The main contribution of probe data is to provide information on (low) speeds that are directly related to supply. Two additional observation models (Obs4 and Obs5) are proposed, where FCD speed observations supplement loop-flow or loop-speed data. The rationale is that the loops give an accurate estimation of the demand-supply volumes along the link (with a good performance) and the FCD speed data judiciously complete the information by providing supplement supply information between detectors. The simulation results also demonstrate that the combination of two data sources provides better estimation results than loop data alone. Note that, travel time estimation with multiple data sources (except for the testing level 3) is not as stable as the estimation with single data sources. This might be caused by coarse data consistency from two sources.

Overall, these results suggest that the current state estimation framework is valid and well performed with the related observation models.

Table 2. $RMSE$ errors of scenarios with different observation models (Obs.) (Speed in m/s, density in veh/m and travel time in second).

	Obs1			**Obs2**			**Obs3**			**Obs4**			**Obs5**		
Test level	*v*	*k*	*TT*	*v*	*k*	*TT*	*v*	*k*	*TT*	*v*	*k*	*TT*	*v*	*k*	*TT*
1	3.66	0.02	3.13	3.69	0.02	3.55	7.06	0.05	*71.33*	3.53	0.03	4.59	3.24	0.03	8.93
2	3.72	0.02	3.41	3.87	0.03	6.00	7.77	0.06	*79.33*	3.64	0.03	6.11	3.41	0.03	8.31
3	**5.35**	0.04	23.65	**6.53**	0.04	14.58	**8.80**	0.06	*88.14*	**4.08**	0.03	20.31	**5.36**	0.04	11.19

Table 3. $MAPE$ errors of scenarios with different observation models (Obs.).

	Obs1			**Obs2**			**Obs3**			**Obs4**			**Obs5**		
Test level	*v*	*k*	*TT*	*v*	*k*	*TT*	*v*	*k*	*TT*	*v*	*k*	*TT*	*v*	*k*	*TT*
1	48.61	16.76	3.86	51.28	11.21	**1.82**	*193.35*	*31.24*	*22.76*	41.45	30.61	4.61	36.62	28.59	3.85
2	50.83	16.14	3.47	53.96	20.83	**2.55**	*232.65*	*34.68*	*26.12*	43.95	28.55	5.03	40.90	28.29	3.61
3	**101.76**	26.82	12.97	**153.58**	18.83	**4.39**	***288.24***	*37.63*	*29.63*	**56.56**	30.19	12.71	**79.19**	17.81	3.69

Table 4. Performance of the Lagrangian-space traffic state estimation with noise in observation and biased model inputs. Noise in Observations (Obs. a~b) : noise power 15~20 dBW. Noise in boundary conditions (Bnd. a~b): noise power 10~15 dBW. Noise in fundamental diagram: FD.a: $v_m = 22\ m/s$, $w = 6\ m/s$ and $k_x = 0.2\ veh/m$; FD.b: $v_m = 21\ m/s$, $w = 5.5\ m/s$ and $k_x = 0.18\ veh/m$.

	Obs1			**Obs2**			**Obs3**			**Obs4**			**Obs5**		
Scenarios	*v*	*k*	*TT*	*v*	*k*	*TT*	*v*	*k*	*TT*	*v*	*k*	*TT*	*v*	*k*	*TT*
Benchmark	3.72	0.02	3.41	3.87	0.03	6.00	7.77	0.06	*79.33*	3.64	0.03	6.11	3.41	0.03	8.31
Obs. a	4.03	0.03	6.75	3.99	0.03	7.99	7.33	0.05	70.22	3.82	0.03	8.09	3.56	0.03	10.28
Obs. b	3.91	0.02	3.60	3.91	0.03	6.25	7.52	0.05	74.28	3.70	0.03	5.57	3.47	0.03	7.88
Bnd. a	3.72	0.02	3.14	3.86	0.03	5.96	7.87	0.06	79.75	3.62	0.03	4.61	3.47	0.03	8.14
Bnd. b	3.72	0.02	3.14	3.82	0.03	5.60	7.90	0.06	80.25	3.62	0.03	4.61	3.46	0.03	8.03
FD. a	**7.08**	**0.05**	**8.12**	**10.00**	**0.06**	**68.42**	**11.38**	**0.07**	**111.09**	**6.59**	**0.05**	**8.20**	**8.91**	**0.06**	**66.53**
FD. b	4.65	0.03	5.07	6.36	0.04	33.39	9.46	0.06	96.92	4.15	0.03	5.28	5.53	0.04	31.87

Table 4 presents the results for the sensitivity study regarding noisy model input and observation input. The benchmark is based on the $RMSE$ error values of scenarios with testing level two from Table 2. Note that for simplicity, the $MAPE$ errors are not presented here but they can demonstrate similar conclusion. Three test categories with two testing variants are identified.

The result indicates that state estimation with noisy observations (both from loop detectors and probe vehicles) and inaccurate initial boundary condition can still provide adequately good estimates. The error indications in two cases are of the same magnitude. This suggests that the influence of the noise can be eliminated in the filtering procedure by appropriately defining error levels for the system model and observation data.

The performance of the state estimation is unsatisfied with biased FD parameters. These parameters are used directly in the process model, and they also indirectly influence the observation model since the current observation depends on the state estimates from the previous (space or platoon) step. Therefore, the performance of the state estimation is quite sensitive to the quality of these relations. With biased model input, it is also noticed that the estimation with (both exclusive and inclusive) loop-flow observations could provide relatively stable estimation results compared with the estimation with speed observations. For operational purposes, observation model 4 might be a more robust solution to implement. In summary, data assimilation techniques can correct random errors (Gaussian white noise) but are sensitivity to biased inputs.

4.2. Qualitative analysis

In the current state estimation framework, the process model evolves state by state, with only one expression to consider all traffic conditions. There involves no complex calculation of the process model in the data-assimilation (correction) step. For instance, there is only one observation for each state correction, resulting in scalar matrix inverse operation and multiplication (see equations (12)-(14)), which is not the case using a space-state form of a system model. This entitles an efficient procedure of data assimilation.

Speed (or flow/density) contour plots can provide intuitive impression of the estimation performance. In all the scenarios (with different observations), the current state estimation approach succeeds to capture the typical traffic patterns (shockwave propagation) presented in the reference case (see Fig. 3). The starting and dissolving time of congestion from estimation are comparable to the ground truth. Furthermore, these plots can demonstrate the improvement of performance by observation data combination (Sce4 and Sce5 compared to Sce1, Sce2 and Sce3).

The travel time is an output that can be easily calculated from mesoscopic results. Fig. 4 presents travel time along the corridor (at different locations) in the scenarios with observation model 5 under three testing levels. The results also indicate travel time estimates can approximate the ground truth values. This is another advantage of the current estimation framework compared to the formulation in other coordinate systems. Travel time estimates require no intermediate transformation from system state variables (e.g., from speed or density in Eulerian or Lagrangian counterparts).

In summary, the proposed formulation of traffic state estimation can deliver adequately good results. The process model provides a time-efficient formulation at the prediction step; and the observation model well fits data measurements into the correction step.

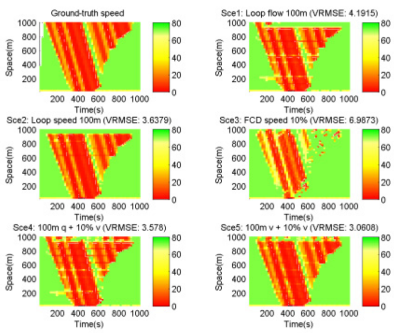

Fig. 3. Speed contour plots of scenarios with five different observation models

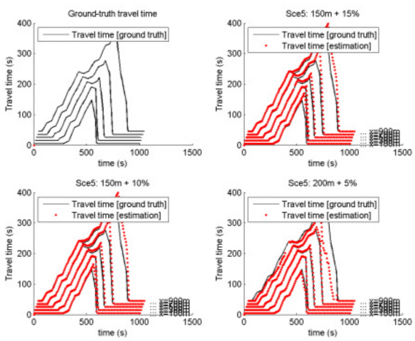

Fig. 4. Travel time estimation in the scenario with observation model 5 under three testing levels.

5. Conclusion and further research

This paper proposes a new mesoscopic traffic state estimation framework using a variational formulation of the LWR model in Lagrangian – space coordinates. The experimental study has demonstrated the feasibility of the proposed framework. As a fundamental and informative indicator in transportation, travel time can be directly derived from the estimation framework. The proposed observation models have been tested and validated for TSE. Observation model 1 provides satisfactory results because the flow observation allows for the modelling of the demand-supply along link boundaries. Observation model 4 outperforms all the other models since it can additionally incorporate the benefits from FCD data and offer stable results when mode input contains calibration errors.

There are several future research directions: (*i*) The current framework applies a continuous lattice implementation, alternatively the selection of spatial cell grid can be dependent on locations of interest and available observation positions to further increase computational efficiency. To be specific, in this paper we apply a grid $\Delta n \times \Delta x$, with $\Delta n = 1$ and $\Delta x = 1/k_x$. The first dimension $\Delta n = 1$ provides individual representation of vehicle, which is convenient for individual travel time estimation or for associating a DTA model to the LWR model (each vehicle follows its own route). The second dimension of the grid is $\Delta x = 1/k_x$. It is not necessary to divide the network into such small cells (that corresponds to the lower bound imposed by the CFL condition). According to the observation model, the necessary condition to be able to assimilate loop data is to have an inter-cell boundary at each loop location. Cell length could be increased without changing the results of the model. It can be convenient to choose a cell size Δx that corresponds to the distance between two consecutive loops. By doing this we can significantly improve the calculation time of the model while keeping the same results. This advantage has been discussed in Section 2.5 and the related validation remains as future work. (*ii*) The current framework only works for a homogeneous road stretch; further research may consider network discontinuity to extend the TSE framework at a network level. (*iii*) Future work is needed to include empirical dataset to test the performance of the method in reality.

References

Herrera, J.C. Bayen, A.M., 2010. Incorporation of Lagrangian measurements in freeway traffic state estimation. Transportation Research Part B: Methodological 44 (4), 460-481.

Wang, Y. Papageorgiou, M., 2005. Real-time freeway traffic state estimation based on extended Kalman filter: A general approach. Transportation Research Part B: Methodological 39 (2), 141-167.

Ngoduy, D., 2008. Applicable filtering framework for online multiclass freeway network estimation. Physica A: Statistical Mechanics and its Applications 387 (2/3), 599-616.

Work, D., Tossavainen, O.-P., Blandin, S., Bayen, A., Iwuchukwu, T. Tracton, K., 2008. An ensemble Kalman filtering approach to highway traffic estimation using GPS enabled mobile devices. Proceedings of the 47th IEEE Conference on Decision and Control, Cancun, Mexico, 2141-2147.

Laval, J.A. Leclercq, L., 2013. The Hamilton-Jacobi partial differential equation and the three representations of traffic flow. Transportation Research Part B: Methodological 52, 17-30.

Leclercq, L., Laval, J. Chevallier, E., 2007. The Lagrangian coordinates and what it means for first order traffic flow models. Proceedings of the 17th International Symposium on Transportation and Traffic Theory, London, 735-753.

Yuan, Y., Van Lint, J.W.C., Wilson, R.E., Van Wageningen-Kessels, F. Hoogendoorn, S.P., 2012. Real-Time Lagrangian Traffic State Estimator for Freeways. IEEE Transactions on Intelligent Transportation Systems 13 (1), 59-70.

Yang, H., Jin, P.J., Ran, B. Yang, D., 2015. Freeway traffic state estimation based on the vehicle (lagrangian)-space traffic flow model: A Lagrangian Kalman filter approach. Proceedings of the Transportation Research Board 94th Annual meeting, Washintong, D.C.

Deng, W., Lei, H. Zhou, X., 2013. Traffic state estimation and uncertainty quantification based on heterogeneous data sources: A three detector approach. Transportation Research Part B: Methodological 57, 132-157.

Newell, G., 1993. A simplified theory of kinematic waves in highway traffic, Part I: General theory. Transportation Research Part B: Methodological 27B (4), 281-287.

Daganzo, C.F., 2005. A variational formulation of kinematic waves: basic theory and complex boundary conditions. Transportation Research Part B: Methodological 39 (2), 187-196.

Leclercq, L., 2007. Hybrid approaches to the solutions of the "Lighthill-Whitham-Richards" model. Transportation Research Part B: Methodological 41, 701-709.

Kalman, R.E., 1960. A new approach to linear filtering and prediction problems. Journal of Basic Engineering 82 (1), 35-45.

LeVeque, R.J., 1992. *Numerical Methods for Conservation Laws.* Basel : Boston : Berlin, Birkhäuser Basel.

Edie, L., 1965. Discussion of traffic stream measurements and definitions. Proceedings of the 2nd International Symposium on Theory of Traffic Flow, Paris, France, 139–154.